The American Journal of Pathology, Vol. 179, No. 5, November 2011

DOI: 10.1016/j.ajpath.2011.07.036

Neurobiology

miRNA Expression Profile after Status Epilepticus and Hippocampal Neuroprotection by Targeting miR-132

Eva M. Jimenez-Mateos,* Isabella Bray,† Amaya Sanz-Rodriguez,* Tobias Engel,* Ross C. McKiernan,* Genshin Mouri,*‡ Katsuhiro Tanaka,*‡ Takanori Sano,*‡ Julie A. Saugstad,§ Roger P. Simon,¶ Raymond L. Stallings,†‖ and David C. Henshall*

From the Departments of Physiology & Medical Physics and Molecular and Cellular Therapeutics–Cancer Genetics,† Royal College of Surgeons in Ireland, Dublin, Ireland; the Department of Neurosurgery,‡ Mie University School of Medicine, Mie, Japan; the Legacy Clinical Research & Technology Center;§ Legacy Research Institute, Portland, Oregon; the Morehouse School of Medicine,¶ Atlanta, Georgia; and the National Children's Research Centre,‖ Our Lady's Children's Hospital, Dublin, Ireland*

When an otherwise harmful insult to the brain is preceded by a brief, noninjurious stimulus, the brain becomes tolerant, and the resulting damage is reduced. Epileptic tolerance develops when brief seizures precede an episode of prolonged seizures (status epilepticus). MicroRNAs (miRNAs) are small, noncoding RNAs that function as post-transcriptional regulators of gene expression. We investigated how prior seizure preconditioning affects the miRNA response to status epilepticus evoked by intra-amygdalar kainic acid in mice. The miRNA was extracted from the ipsilateral CA3 subfield 24 hours after focal-onset status epilepticus in animals that had previously received either seizure preconditioning (tolerance) or no preconditioning (injury), and mature miRNA levels were measured using TaqMan low-density arrays. Expression of 21 miRNAs was increased, relative to control, after status epilepticus alone, and expression of 12 miRNAs was decreased. Increased miR-132 levels were matched with increased binding to Argonaute-2, a constituent of the RNA-induced silencing complex. In tolerant animals, expression responses of >40% of the injury-group-detected miRNAs differed, being either unchanged relative to control or down-regulated, and this included miR-132. *In vivo* microinjection of locked nucleic acid-modified oligonucleotides (antagomirs) against miR-132 depleted hippocampal miR-132 levels and reduced seizure-induced neuronal death. Thus, our data strongly suggest that miRNAs are important regulators of seizure-induced neuronal death. ***(Am J Pathol 2011, 179:2519–2532; DOI: 10.1016/j.ajpath.2011.07.036)***

The brain possesses endogenous molecular mechanisms by which it can protect itself from harm, although forewarning is required to bring protection optimally to bear. Thus, mild noxious stressors such as brief ischemia or brief seizures evoke protective adaptations in the brain, which render it powerfully refractory against a subsequent and otherwise damaging insult.[1–3] The effect of the stressor has been termed preconditioning, and the protected state after the damaging insult is termed tolerance. Our understanding of the molecular processes underlying tolerance has been helped by microarray profiling. Such profiling has revealed large-scale, genomic reprogramming of the response to injury involving altered expression of hundreds of genes.[4,5] The prominent transcriptional response in tolerant brain is gene down-regulation.[6–8] In ischemic tolerance, the most affected processes are metabolism, transport, and inflammation,[6,7] whereas the genes altered in epileptic tolerance encode ion channels, excitatory neurotransmitter receptors, and calcium signaling components.[8]

The mechanism by which gene expression is altered in tolerance is unknown, but a contribution by microRNAs (miRNAs) has recently been proposed.[9–11] The miRNAs

Supported by Science Foundation Ireland grant 08/IN1/B1875 (D.C.H.), Health Research Board grant PHD/2007/11, a postdoctoral fellowship from the Irish Research Council for Science Engineering and Technology (E.J.-M.), the National Biophotonics and Imaging Platform Ireland, and the Children's Medical and Research Foundation.

Accepted for publication July 12, 2011.

Supplemental material for this article can be found at *http://ajp.amjpathol.org* or at doi: 10.1016/j.ajpath.2011.07.036.

Address reprint requests to David C. Henshall, Ph.D., Department of Physiology & Medical Physics, Royal College of Surgeons in Ireland, 123 St. Stephen's Green, Dublin 2, Ireland. E-mail: dhenshall@rcsi.ie.

are a family of small (~22 nucleotides), endogenously expressed, noncoding RNAs that regulate mRNA translation by imperfect base-pairing interactions within the 3′ untranslated region (UTR).[12] Several hundred miRNAs have been identified in mammals, and miRNAs may be capable of regulating post-transcriptional expression of one-third or more of the protein-coding genes.[13–15] Biogenesis begins with transcription by either RNA polymerase II or III to generate a pri-miRNA. Nuclear processing via Drosha, an RNase III endonuclease, produces a pre-miRNA that is then exported to the cytoplasm for processing by Dicer to the mature double-strand miRNA.[16,17] One strand is then loaded into the RNA-induced silencing complex, which contains argonaute proteins and, depending on sequence complementarity, directs mRNA degradation or translational repression of the target mRNA.[18]

The miRNA system exhibits dynamic spatiotemporal expression during brain development.[19,20] Physiological and pathological neuronal activity also modulate expression of miRNA genes,[21,22] and miR-132 (along with other miRNAs) regulates neuronal structure.[23–26] Loss of biogenesis components (eg, Dicer) results in neurodegeneration within some, but not all, brain regions.[27–29] Roles for miRNA dysfunction have been proposed in acute neurological injury and neurodegenerative diseases.[30,31]

In the present study, we used expression profiling to examine how the miRNA response to status epilepticus evoked by intra-amygdalar kainic acid (KA) is altered in a model of epileptic tolerance previously developed by our group.[32] We then used a small-molecule-inhibitor approach to model the changes brought on by tolerance and to test whether miRNAs contribute *in vivo* to seizure-induced neuronal death.

Materials and Methods

Animal Model of Epileptic Tolerance

All animal experiments were performed in accordance with European Communities Council Directive 86/609/EEC and were reviewed and approved by the Research Ethics Committee of the Royal College of Surgeons in Ireland, under license from the Department of Health, Dublin, Ireland. Adult male C57BL/6 mice (20 to 22 g) from Harlan (Oxon, Bicester, UK) were used. Control mice received a single intraperitoneal injection of 0.2 mL saline on day 1 (sham preconditioning), followed by intra-amygdalar vehicle on day 2 (0.2 μL PBS). Injury group mice also received intraperitoneal injection of 0.2 mL saline on day 1, and then underwent status epilepticus induced by intra-amygdalar KA (Sigma-Aldrich, Dublin, Ireland; St. Louis, MO) on day 2. Tolerance mice underwent seizure preconditioning on day 1 via intraperitoneal injection of 0.2 mL KA (15 mg/kg), and then underwent status epilepticus on day 2 induced by intra-amygdalar KA.

Surgical Procedures

For intra-amygdalar injections, mice were anesthetized with isoflurane (5% induction, 1% to 2% maintenance) and placed in a mouse-adapted stereotaxic frame. Body temperature was maintained within the normal physiological range with a rectal thermometer and feedback-controlled heat pad (Harvard Apparatus, Kent, UK; Holliston, MA). After a midline scalp incision, the bregma was located and three partial craniectomies were performed for placement of skull-mounted recording screws (Bilaney Consultants, Sevenoaks, Kent, UK). A complete craniectomy was drilled for placement of a guide cannula for intra-amygdalar injections (coordinates from bregma: AP = −0.94 mm, L = −2.85 mm), based on a stereotaxic atlas.[33] The cannula and electrode assembly was fixed in place with dental cement and the animal was placed in a recording chamber. The electroencephalogram (EEG) was recorded using a Grass Comet XL laboratory-based EEG system (Grass Technologies, Slough, UK; West Warwick, RI). After baseline EEG recordings, the animal was lightly restrained while an injection cannula was lowered 3.75 mm below the brain surface for injection of KA (1 μg) or vehicle in a volume of 0.2 μL into the basolateral amygdala nucleus. After 40 minutes, all mice received lorazepam (Ativan; 6 mg/kg, i.p.). Animals were recorded for up to 1 hour thereafter, before being disconnected and placed in a warmed recovery chamber.

For intracerebroventricular injections, additional mice were affixed with a cannula ipsilateral to the site of KA injection, as described previously.[34] Coordinates from the bregma were AP = −0.3 mm, L = −1.0 mm, V = −2.0 mm. Mice received 2 μL infusion of either scrambled or miR-132 antagomir (locked nucleic acid LNA- and 3′-cholesterol-modified oligonucleotides; Exiqon, Vedbaek, Denmark) in artificial cerebrospinal fluid (Harvard Apparatus). Twenty-four hours later, mice were either euthanized or were subjected to status epilepticus, as described above.

Mice were euthanized at 24 hours after intra-amygdalar injections. Animals were given a pentobarbital overdose and were perfused with ice-cold saline to remove intravascular blood components. Brains for molecular and biochemical work were dissected on dry ice under a microscope and the hippocampus was subdivided to obtain the separate CA3-enriched portion, as described previously.[8] For histology, mice were first perfused with ice-cold saline and then either perfusion-fixed with paraformaldehyde (4%) or brains were fresh-frozen in 2-methylbutane at −30°C.

Electroencephalography Analysis

EEGs were analyzed using TWin software v3.8 (Grass Technologies), and the duration of high-amplitude, high-frequency discharges (also termed type IV seizures) was calculated between the time of KA injection and the time of lorazepam administration.[35] Additional frequency and amplitude analysis of EEG was performed using LabChart Pro version 7 software (ADInstruments, Oxford, UK).

miRNA Extraction and Expression Profiling of Pooled miRNAs

Total mRNA was extracted using an miRNeasy kit (Qiagen, West Sussex, UK; Valencia, CA) according to the manufacturer's instructions to obtain an enrichment of small RNAs. For each condition, ipsilateral CA3 subfields from three separate mice were pooled together for analysis, and this was repeated using independent samples. Quality and quantity of mRNA was measured using a NanoDrop spectrophotometer (Thermo Scientific, Loughborough, UK; Wilmington, DE), and RNA dilutions were made up in nuclease-free water. Reverse transcription of 250 ng of miRNA from the CA3 subfields from each condition was performed using stem-loop multiplex primer pools (Applied Biosystems, Paisley, UK; Foster City, CA), allowing reverse transcription of 48 different miRNAs in each of eight RT pools. The miRNA quantitative PCR (qPCR) screen was performed on the 7900HT fast real-time system using TaqMan low-density arrays (TaqMan TLDA MicroRNA assays version 1.0 containing 380 human microRNAs assays; Applied Biosystems). Of the profiled human miRNAs, 197 were 100% homologous to mouse. miRNAs were considered differentially expressed at a threshold of $\pm$1.5-fold.[36]

Stem-Loop Reverse Transcription and Real-Time qPCR of Individual miRNAs

Reverse transcription for individual qPCRs was performed using 250 ng of total RNA and a high-capacity reverse transcription kit (Applied Biosystems); RT-specific primers for mouse miRNAs miR-27a, miR-92a, miR-101, miR-127, miR-132, miR-145, miR-200a, and miR-326 (Applied Biosystems) were used for all miRNA reverse transcription. Individual qPCRs were performed on the 7900HT fast real-time system (Applied Biosystems) using miR-27a, miR-92a, miR-101, miR-127, miR-132, miR-145, miR-200a, and miR326-specific TaqMan microRNA assays (Applied Biosystems). RNU19 was used for normalization miRNA expression studies, as described previously.[37] A relative fold change in expression of the target gene transcript was determined using the comparative cycle threshold method ($2^{-\Delta\Delta CT}$).

Western Blotting

Western blot analysis was performed as described previously.[38] Hippocampal CA3 subfields were homogenized in a lysis buffer, boiled in gel-loading buffer, separated on SDS-PAGE gels, and transferred onto nitrocellulose membranes. The following primary antibodies were used: Drosha (1:400; Cell Signaling Technology, Danvers, MA), Dicer-1 (1:400; Santa Cruz Biotechnology, Santa Cruz, CA), Argonaute-2 (Ago-2) (1:400; Cell Signaling Technology), and Tubulin (1:2000, Sigma-Aldrich). Membranes were then incubated with horseradish peroxidase-conjugated secondary antibodies (Jackson ImmunoResearch, West Grove, PA) and bands were visualized using Pierce SuperSignal West Pico chemiluminescence substrate (Thermo Fisher Scientific, Rockford, IL). Images were captured using a Fuji-Film LAS-300 (Fuji, Sheffield, UK), and densitometry was performed using AlphaEaseFC4.0 gel-scanning integrated optical density software (Alpha Innotech; ProteinSimple, San Leandro, CA).

Immunoprecipitation of Argonaute-2 (Ago-2)

Pools of three individual mouse CA3 subfields from each condition were homogenized in 0.7 mL of ice-cold immunoprecipitation buffer (300 mmol/L NaCl, 5 mmol/L $MgCl_2$, 0.1% NP-40, 50 mmol/L Tris-HCl pH 7.5). The homogenate was centrifuged at 16,000 $\times$ *g* for 15 minutes at 4°C and the supernatant was considered as the total cell lysate. Five micrograms of anti-Ago-2 was added to each 400 μg of supernatant in a final volume of 1 mL. The solution was vortex-mixed and incubated overnight at 4°C. After addition of 20 μL of 50% protein-A/G-agarose beads (Santa Cruz Biotechnology), the solution was mixed and incubated for 1 hour at 4°C. The beads were centrifuged at 16,000 $\times$ *g* for 15 minutes at 4°C, and the supernatant was removed. The pellet was washed twice with immunoprecipitation buffer, and miRNA was extracted using an miRNeasy kit (Qiagen, West Sussex, UK). Stem-loop reverse transcription and real-time qPCR (Applied Biosystems) was performed as described above to semiquantify the expression of the miRNA.

Histopathology

To characterize seizure-damage in the model, brains from control, injury, and tolerance mice were sectioned at 12 μm on a cryostat (−20°C) at the level of either rostral (AP = −1.58 mm) or medial (AP = −1.82 mm) hippocampus.[33] Fluoro-Jade B (FJB) staining was performed as described previously.[8,39] Briefly, tissue sections were allowed to air-dry and then were postfixed in formalin (10%), immersed in 0.006% potassium permanganate solution, rinsed again, and then transferred to FJB solution (0.001% in 0.1% acetic acid) (Millipore-Chemicon Europe, Chandlers Ford, UK; Billerica, MA). Sections were then rinsed again, dried, cleared, and mounted in DPX mounting medium (Sigma-Aldrich). Analysis of DNA damage was performed on fresh-frozen sections using a fluorescein-based TUNEL technique, according to the manufacturer's instructions (Promega, Madison, WI) and as described previously.[38]

For assessment of neuron loss, sections were fixed, blocked in 5% goat serum, and incubated with antibodies against neuronal nuclear protein (1:500 NeuN; Millipore Ireland, Tullagreen, Cork, Ireland), which was detected using goat anti-mouse Alexa Fluor 568 (Bio-Sciences, Dun Laoghaire, Ireland). Sections were examined using a Nikon 2000s epifluorescence microscope (Micron Optical, Enniscorthy, Ireland) under excitation/emission (Ex/Em) wavelengths of 472/520 nm (green) and 540 to 580/600 to 660 nm (red). Pseudocolor transforms from monochromatic images acquired using an Orca-285 digital camera (Hamamatsu Photonics, Hamamatsu City, Japan) were generated using Adobe Photoshop version

6.0 software. Cell counts were performed for the entire CA3 subfield, beginning at the border with CA2 through to the end of CA3c/CA4 within the hilus of the dentate gyrus. Counts of FJB-, TUNEL- and NeuN-stained cells were the average of two adjacent sections assessed by an observer blinded to experimental group and condition.

In Situ *Hybridization*

For *in situ* hybridization, mice ($n = 3$) were perfused with ice-cold PBS followed by paraformaldehyde (4%). Sections (12 μm thick) were mounted on SuperFrost-Plus slides (VWR International, Radnor, PA) and air dried. Using RNase free solutions, slides were washed with PBS and radioimmunoprecipitation assay buffer [150 mL NaCl, 1% (octylphenoxy)polyethoxyethanol (IGEPAL)], 0.5% sodium deoxycholate, 0.1% SDS, 1 mmol/L EDTA, 50 mmol/L Tris pH 8.0) for 5 minutes, then treated with 4% paraformaldehyde for 10 minutes. Sections were washed again and treated with 0.25% acetic anhydride/0.1 mol/L triethanolamine, then rinsed with 0.1% Tween-20/PBS for 5 minutes, treated with 5 μg/mL proteinase K for 4 minutes, and washed with PBS. Next, slides were rinsed in prehybridization buffer (1× saline solution, 50% formamide, and 1× Denhardt's solution) for 1 hour at 56°C (melting temperature $T_m = -20$°C, as specified by Exiqon). The probe to detect mi-132 was 5′-digoxigenin-labeled, 2′-*O*,4′-*C*-methylene bicyclonucleoside monomer-containing oligonucleotide (LNA-modified). The sequence was the reverse complement to the mature miRNA. Probes were incubated 1:200 in hybridization buffer (1× saline solution, 50% formamide, and 1× Denhardt's plus 10% dextran sulfate) overnight at 56°C in a humidified chamber. On the next day, sections were washed in FAM buffer (2× SSC, 50% formamide, and 0.1% Tween 20) for 1 hour at 60°C. Then sections were rinsed in B1 buffer (150 mmol/L NaCl, 100 mmol/L maleic acid, and 0.4% IGEPAL pH, 7.5) for 1 hour at room temperature and in B2 buffer (2% blocking reagent and 10% goat serum in B1 buffer) for 30 minutes. Anti-DIG-PA antibody (1:1000; Roche Applied Science, Indianapolis, IN) was incubated in B2 buffer overnight at 4°C. On the next day, sections were washed in B1 buffer and incubated in B3 buffer (100 mmol/L NaCl, 50 mmol/L $MgCl_2$, 0.025% Tween 20 and 100 mmol/L Trizma pH9.5) for 30 minutes. Then, 200 μL of color substrate solution [nitroblue tetrazolium/5-bromo-4-chloro-3-indolyl phosphate (BNT/BCIP stock solution; Roche Applied Science)] diluted 1:50 in B3 buffer was added to each slide until the signal appeared. Slides were then rinsed, mounted, and coverslipped.

Statistical Analysis

All data are presented as means ± SEM. Two-group comparisons were made using Student's *t*-test; multigroup comparisons were made using analysis of variance followed by appropriate post hoc testing. Significance was set at $P < 0.05$.

Results

Reduced Hippocampal CA3 Damage after Status Epilepticus in Epileptic Tolerance

In our experimental paradigm (Figure 1A), status epilepticus was focally evoked by intra-amygdalar KA. This approach avoids direct neurotoxin-associated effects that could complicate attributing miRNA changes to seizures alone (eg, in models in which KA is injected either systemically or intrahippocampally). The histopathological features of the tolerance model were as previously reported.[8,32,39] In non-preconditioned mice subjected to status epilepticus (ie, in the injury group), the ipsilateral hippocampal CA3 subfield was extensively damaged, as evidenced by FJB staining at 24 hours (Figure 1, B and D). In this model, only few FJB-positive cells are found in the ipsilateral CA1 subfield (Figure 1D). FJB staining was consistently found within the CA4/hilar region of the dentate gyrus, but not in the granule cell layer (Figure 1D). Hippocampal CA3 damage was significantly reduced in mice given seizure preconditioning 24 hours before status epilepticus (tolerance group; Figure 1, B and D). The duration of high-amplitude, high-frequency electrographic seizures did not show a significant difference between injury and tolerance mice (Figure 1, E and F). Thus, seizure preconditioning reduces hippocampal damage independently of changes to the overall severity of the status epilepticus.

Because in this model the CA3 subfield was the major site for both damage and protection from damage, we performed all biochemical and molecular studies on the isolated CA3 subfield. This was achieved by microdissection (as described under *Materials and Methods*) with minimized contamination of undamaged or minimally injured fields that might obscure or dilute miRNA changes. CA3 samples were confirmed as being enriched by real-time qPCR analysis of the CA3-specific gene *bok*,[40] which was present in CA3 but nearly absent from CA1 samples (Figure 1C).

miRNA Biogenesis Pathway in Injury and Tolerance

To establish the presence of miRNA biogenesis pathway components in the model, we examined expression of Dicer, Drosha, and Ago-2 by Western blotting. Each protein was present in the CA3 subfield in control, injury, and tolerance mice at 24 hours. All three proteins were present at the predicted molecular weight: Drosha at ~160 kDa, Dicer at ~220 kDa, and Ago-2 (also known as eukaryotic translation initiation factor 2C 2) at ~90 kDa (Figure 2A). Protein levels of each were not significantly altered in animals subjected to status epilepticus (Figure 2B).

Hippocampal CA3 miRNA Transcriptome after Status Epilepticus

We next compared the mature miRNA expression profile of the CA3 subfields from control animals, mice subjected to status epilepticus without preconditioning (injury group), and mice given seizure preconditioning 24 hours before status epilepticus (tolerance group). A heat

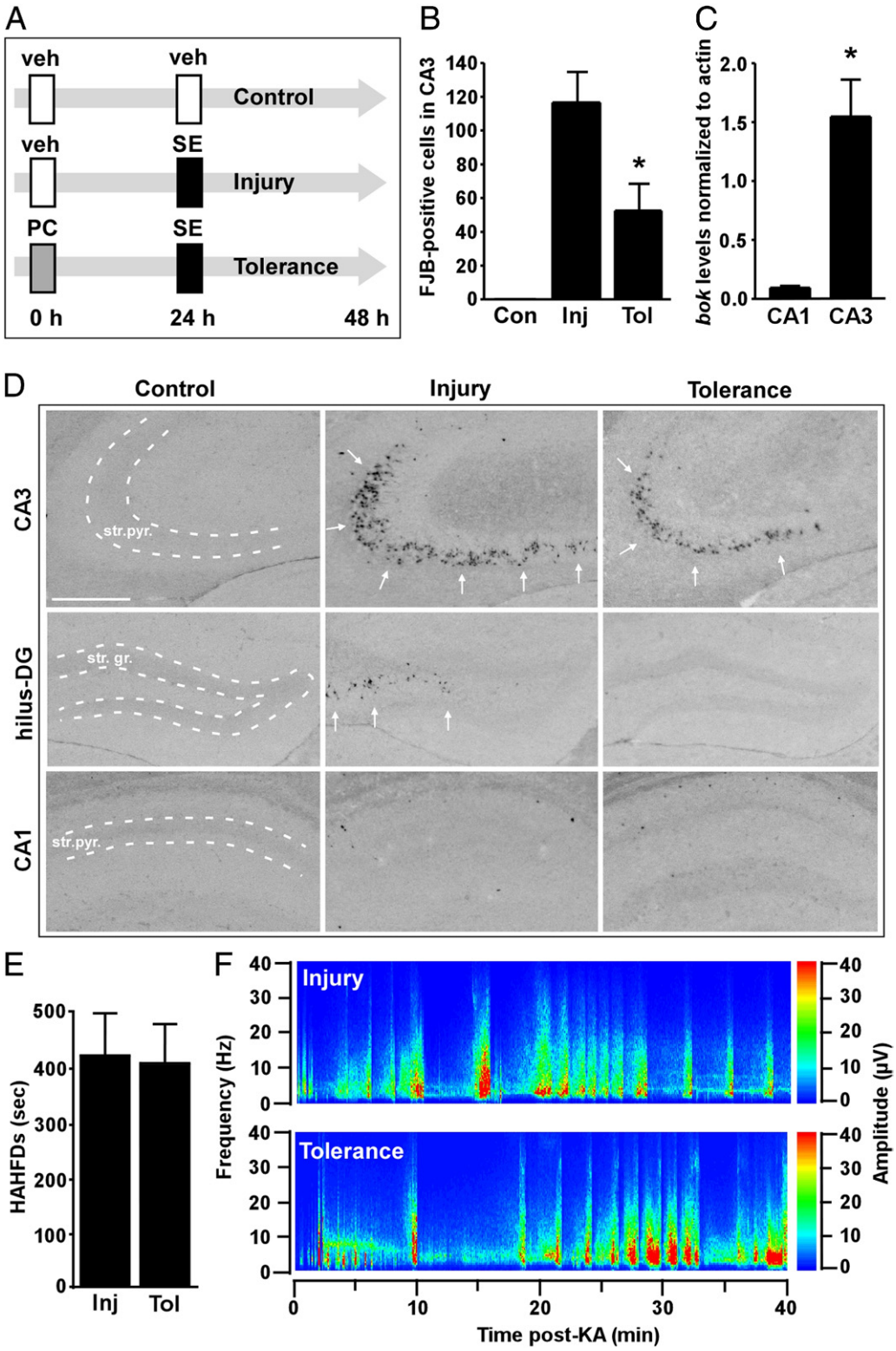

Figure 1. Epileptic tolerance is associated with reduced damage to the CA3 subfield. **A:** Schematic of the experimental paradigm. On day 1, animals receive intraperitoneal injection of either vehicle (veh) or seizure preconditioning [PC; 15 mg/kg kainic acid (KA), i.p.]. On day 2, mice receive intra-amygdalar injection of either vehicle or kainic acid (1 μg) to induce status epilepticus (SE), and on day 3 brains are extracted. **B:** Fluoro-Jade B (FJB) positive cell counts in the ipsilateral CA3 subfield 24 hours after status epilepticus in mice in the injury (Inj), tolerance (Tol), and nonseizure control (Con) groups ($^*P < 0.05$ versus Inj, $n = 4$ per group). **C:** *Bok* enrichment in the microdissected CA3 subfield compared with CA1 ($^*P < 0.05$ versus CA1, $n = 3$ per group). **D:** Representative photomicrographs showing FJB staining at 24 hours in each group within (**top**) CA3, (**middle**) hilus-dentate gyrus (DG) and (**bottom**) CA1. Note the reduction in numbers of damaged neurons (**arrows**) in tolerance mice in the CA3 and hilus-DG regions, compared with injury mice. str. pyr., stratum pyramidale; str. gr., stratum granulosum. Original magnification, ×4. Scale bar, 500 μm. **E:** Duration of high-amplitude, high-frequency discharges (HAHFDs) in injury and tolerance mice during status epilepticus. **F:** EEG during status epilepticus for each group from representative animals showing similarity of frequency and amplitude.

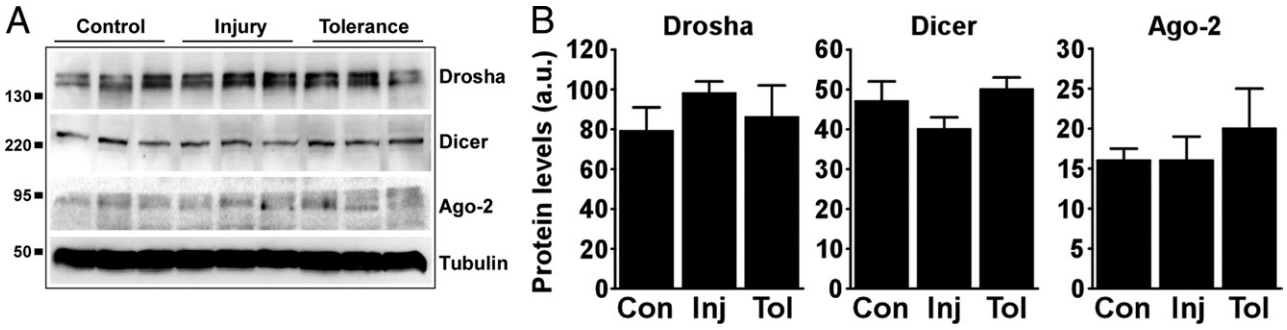

Figure 2. miRNA biogenesis components in injury and tolerance. **A:** Immunoblots of CA3 subfield whole-cell lysates from control, injury, and tolerance mice (n = 1 per lane) obtained 24 hours after intra-amygdalar injections show expression of Dicer, Drosha, and Ago-2. α-Tubulin is included as a guide to protein loading. **B:** Densitometry for each protein. Values are in arbitrary units. n = 3 per group.

map shows the patterns of miRNA expression among the three different experimental groups (Figure 3A). A total of 45 mature miRNAs were called as present in the CA3 subfield of nonseizure control mice on the basis of qPCR detection in two independent experiments under the cut-off point (≤35 cycle times).

There were prominent changes to miRNA expression in mice subjected to status epilepticus alone (Figure 3A and Table 1). Compared with control, 54% of miRNAs were increased in expression after status epilepticus and ~21% were decreased (Figure 3B). Expression of ~25% of the remaining detected miRNAs was unchanged after status epilepticus (Figure 3B). All miRNAs present in the injury group were also detected in control animals, whereas miR-518b, miR-518c, miR-520c, and miR-520g were below cutoff in both injury and tolerance mice. The miRNAs showing altered expression after status epilepticus are listed in Table 1. The median miRNA up-regulation in injury was 5.4-fold; however, the scale of miRNA up-regulation was dramatic for several miRNAs, including >20-fold for miR-132, miR-219 and miR-323 and between ~45-fold and ~144 fold for miR-21, miR-507, and

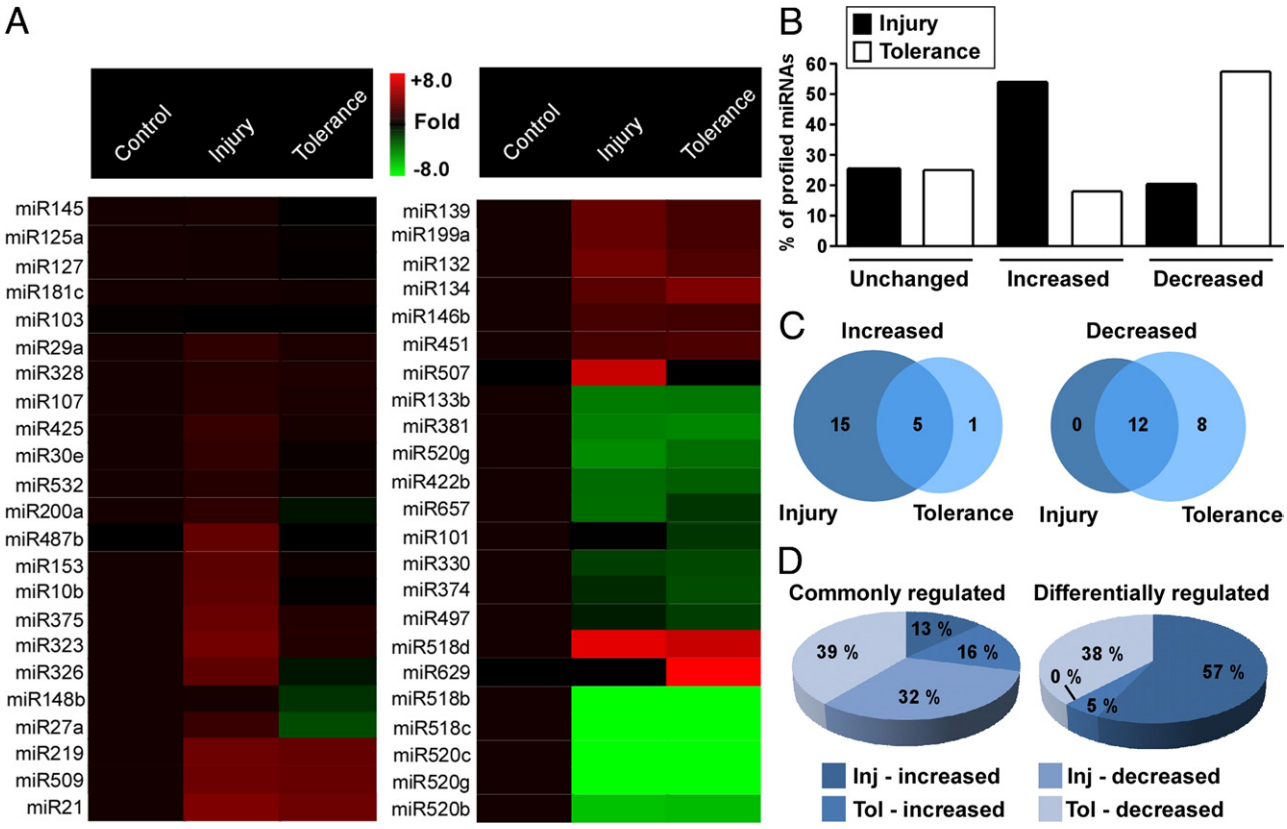

Figure 3. miRNA expression profile in injury and tolerance mice. **A:** Heat map depicting miRNA expression data for each group relative to control. Fewer miRNAs were up-regulated and more were down-regulated in tolerance mice, compared with injury mice. **B:** Percentage of the detected miRNAs in each seizure group as unchanged, up-regulated, or down-regulated, relative to control. **C:** Numbers of miRNAs and their overlap between injury and tolerance groups for those increased and decreased, relative to control. **D:** Percentage of up-regulated and down-regulated miRNAs that were commonly or differentially regulated between injury (Inj) and tolerance (Tol).

Table 1. Differential miRNA Expression in Injury and Tolerance, Relative to Control

miRNA	Injury	Tolerance	miRNA	Injury	Tolerance
miR10b	8.54	1.0	miR326	6.93	−5.27
miR21	44.58	21.66	miR328	1.4	1.22
miR-27a	2.5	−3.31	miR330	−3.89	−7.69
miR29a	1.86	1.18	miR374	−2.76	−10.1
miR30e	1.92	0.78	miR375	12.31	1.10
miR101	0.8	−3.5	miR381	−4.76	−6.58
miR103	0.99	−1.77	miR422b	−4.33	−2.70
miR107	1.01	−2.35	miR425	2.16	1.05
miR125a	0.9	0.7	miR451	3.44	4.33
miR127	0.93	−1.50	miR487b	1.46	1.15
miR132	22.2	1.15	miR497	−2.35	−3.67
miR133b	−3.76	−3.11	miR507	76.91	1.0
miR134	2.49	2.21	miR509	7.89	13.93
miR139	6.56	1.06	miR518b	n.d	ND
miR145	1.15	−1.61	miR518c	n.d	ND
miR146b	3.91	1.22	miR518d	143.92	70.40
miR148b	1.01	−2.16	miR520b	−52.63	−39.21
miR153	6.65	0.85	miR520c	n.d	ND
miR181c	1.01	0.90	miR520g	n.d	ND
miR199a	7.50	1.49	miR532	1.47	0.83
miR200a	6.99	−3.14	miR629	1.0	2229
miR219	22.96	5.16	miR657	−22.2	−3.57
miR323	22.62	1.38			

The miRNA was extracted from the ipsilateral CA3 subfield 24 hours after focal-onset status epilepticus in animals that had previously received either seizure preconditioning (tolerance) or no preconditioning (injury). Values represent the fold difference relative to control for miRNAs expressed in injury and tolerance.

ND, not detected (expression in injury and tolerance was below the 35 cycle cutoff).

miR-518d. The median miRNA down-regulation was a 3.6-fold decrease; however, the range between the down-regulated miRNAs included 22-fold decrease for miR-657 and >50-fold decrease for miR-520b.

Altered miRNA Profile in Epileptic Tolerance

The miRNA response to status epilepticus in preconditioned mice differed in several aspects from that generated by status epilepticus alone (Figure 3 and Table 1). Only a fraction (18%) of miRNA expression was increased in epileptic tolerance, compared with the control; a much larger proportion was down-regulated (~60%). The proportion of miRNAs that remained unchanged relative to control was similar to that of the injury group (~25%) (Figure 3B). One miRNA (miR-629) was uniquely expressed in epileptic tolerance samples, but it was outside the 35-cycle cutoff point in the control and injury groups.

The overlap between injury and tolerance for up-regulated and down-regulated miRNAs is shown as Venn diagrams in Figure 3C. Five miRNAs were up-regulated in both injury and tolerance groups; 15 miRNAs were uniquely up-regulated in the injury group and 1 miRNA was uniquely up-regulated in the tolerance group. Among the up-regulated miRNAs common to both groups, the scale of increase was usually greater in the injury than in the tolerance group.

Among down-regulated miRNAs, 12 were common to both injury and tolerance groups (Figure 3, C and D). There were no uniquely down-regulated miRNAs in the injury group (Figure 3, C and D). In the tolerance group, eight miRNAs were uniquely down-regulated. The scale of down-regulation was typically greater in tolerance than injury for a given miRNA (Table 1).

Of particular note, a subset of miRNAs displayed opposite regulation between injury and tolerance. Expression of miR-27a, miR-200a, and miR-326 were all increased after status epilepticus alone, but were decreased in epileptic tolerance.

Validation of TaqMan Screen

To validate the TLDA card results, we chose a selection of miRNAs from among those up-regulated in injury (miR-132, miR-200a, and miR-326) and those down-regulated in tolerance (miR-101, miR-127 and miR-145) for individual real-time qPCR verification using miRNA specific primers (as described in *Materials and Methods*). Individual qPCR validation of the screening results showed high reproducibility (Figure 4 and Figure 5B). However, the scale of the fold increase or decrease tended to be at variance between the two methods. In particular, the very high levels of up-regulation seen for some miRNAs with the TLDA approach were more limited with the individual qPCR. One miRNA reported to be up-regulated in injury on the TLDA analysis

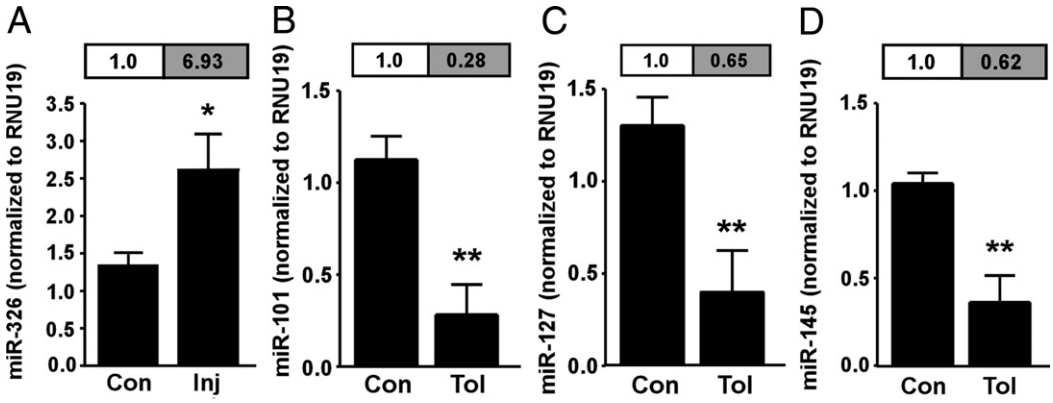

Figure 4. Real-time qPCR analysis of miRNA expression responses in injury and tolerance. Expression (mature levels) of miR-326 (**A**), miR-101 (**B**), miR-127 (**C**), and miR-145 (**D**) at 24 hours for injury (Inj) or tolerance (Inj) mice, compared with control (Con). Data were corrected to levels of RNU19. Fold-change values (**boxed**) were obtained from the TaqMan low-density array profiling experiment for comparison. $n = 4$ per group. $^{*}P < 0.05$; $^{**}P < 0.01$ versus Con.

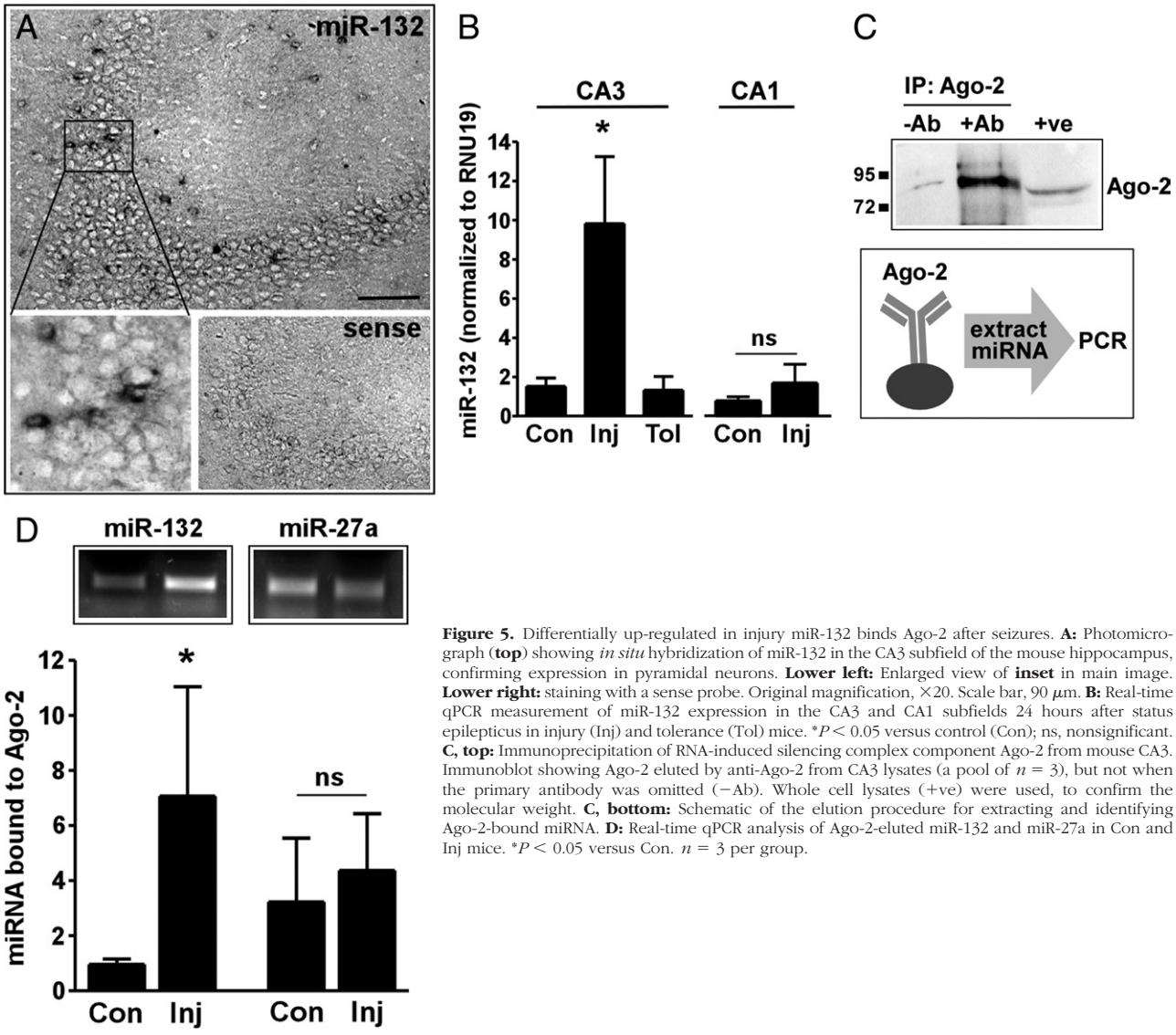

Figure 5. Differentially up-regulated in injury miR-132 binds Ago-2 after seizures. **A:** Photomicrograph (**top**) showing *in situ* hybridization of miR-132 in the CA3 subfield of the mouse hippocampus, confirming expression in pyramidal neurons. **Lower left:** Enlarged view of **inset** in main image. **Lower right:** staining with a sense probe. Original magnification, ×20. Scale bar, 90 μm. **B:** Real-time qPCR measurement of miR-132 expression in the CA3 and CA1 subfields 24 hours after status epilepticus in injury (Inj) and tolerance (Tol) mice. $^*P < 0.05$ versus control (Con); ns, nonsignificant. **C, top:** Immunoprecipitation of RNA-induced silencing complex component Ago-2 from mouse CA3. Immunoblot showing Ago-2 eluted by anti-Ago-2 from CA3 lysates (a pool of $n = 3$), but not when the primary antibody was omitted (−Ab). Whole cell lysates (+ve) were used, to confirm the molecular weight. **C, bottom:** Schematic of the elution procedure for extracting and identifying Ago-2-bound miRNA. **D:** Real-time qPCR analysis of Ago-2-eluted miR-132 and miR-27a in Con and Inj mice. $^*P < 0.05$ versus Con. $n = 3$ per group.

(miR-200a) was not confirmed by individual qPCR (1.2 ± 0.3 fold change in injury compared with control, $P > 0.05$).

Increased Binding of miR-132 to Ago-2 after Status Epilepticus

Among the differentially expressed miRNAs, the predominance of up-regulation among injury genes and down-regulation or lack of change in tolerance implies that neuroprotection may be due in part to reduced levels of certain miRNAs. We selected miR-132 (Table 1) as a candidate for further analysis because the strong up-regulation seen in injury was completely prevented in tolerance, and also because it is has been shown to have a role in regulating neuronal structure,[23,26,41] but has not previously been linked to control of neuronal death.

In situ hybridization was first used to confirm that miR-132 is constitutively expressed in CA3 pyramidal neurons in the mouse hippocampus (Figure 5A). Next, using individual real-time qPCR we confirmed that miR-132 was up-regulated in the CA3 subfield after status epilepticus alone, but levels were the same as control in seizure-preconditioned mice subjected to status epilepticus (Figure 5B). We also examined the expression of miR-132 in the CA1 subfield, which is not significantly damaged in the injury model. In contrast to findings for CA3, miR-132 was not up-regulated in the CA1 subfield after status epilepticus alone (Figure 5B).

Ago-2 both contributes to miRNA-mRNA pairing and influences whether mRNA stability is reduced or mRNA is cleaved.[16–18] We next asked whether increased levels of mature miRNA also lead to increased loading into the RNA-induced silencing complex. Accordingly, we examined miR-132 association with Ago-2 using CA3 samples from the injury group. Ago-2 was readily immunoprecipitated from hippocampal CA3 lysates (Figure 5C). Ago-2 was then immunoprecipitated from control and seizure-damaged CA3 subfields at 24 hours and bound miRNA was extracted (Figure 5C). Ago-2-eluted miR-132 was then identified by PCR. miR-132 was present at low levels in Ago-2

immunoprecipitates in control CA3 lysates (Figure 5D). Levels of miR-132 were significantly increased in Ago-2 samples from seizure-damaged mice (Figure 5D). As a control for the specificity of the miR-132 finding, we analyzed expression of miR-27a, a second seizure-up-regulated miRNA. miR-27a was also detected after Ago-2 pull-down assay, but levels were not increased relative to control (Figure 5D). Thus, increased loading of miRNAs into Ago-2 is not typical for all seizure-up-regulated miRNAs.

In Vivo *Depletion of miR-132 Using Antagomirs*

To determine whether miR-132 contributed to neuronal death after seizures *in vivo*, we used locked nucleic acid (LNA)-modified and 3′ cholesterol-conjugated anti-miR-132 oligonucleotides (ie, antagomirs) to reduce brain levels of miR-132 before status epilepticus. Previous work has shown that antagomirs cause a pronounced reduction of their miRNA targets.[42–44] In our experiments, miR-132 antagomirs or a nontargeting scrambled version were injected intracerebroventricularly into mice at various doses. Effective miRNA depletion was confirmed by extracting the CA3 subfield of the hippocampus and measuring miRNA levels by individual real-time qPCR. A dose of 0.5 nmol antagomir significantly reduced miR-132 levels at 24 hours, whereas 0.12 nmol had no effect (Figure 6A). The same dose (0.5 nmol) of scrambled antagomir had no effect on miR-132 levels. Suppression of miR-132 was greater when 1.0 nmol of antagomir was injected (Figure 6A); however, the matching dose of scrambled antagomir also depleted miR-132 from brain (Figure 6A). As a further control, we examined the effects of miR-132 antagomirs and scrambled antagomirs on the levels of miR-92a, an unrelated miRNA (Figure 6B). Injection of 0.12 or 0.5 nmol of miR-132 antagomir or scrambled antagomir did not alter expression of miR-92a (Figure 6B). In contrast, at the highest dose of scrambled antagomir (1.0 nmol), but not of miR-132-targeting antagomirs, levels of miR-92a were significantly reduced ($P < 0.0001$; Figure 6B).

Effects of Antagomirs on the Hippocampus and EEG Parameters

To determine whether anti-miR-132 or scrambled antagomir injection had any general cytotoxic effects, we performed neuron counts and stained for FJB and irreversible DNA damage using TUNEL.[38] Counts of NeuN-immunostained sections at the level of rostral and medial hippocampus from mice injected 24 hours earlier with 0.5 nmol of the antagomirs revealed no neuron loss (Figure 6C). No FJB staining was evident in hippocampal sections from mice injected with either scrambled or miR-132 antagomir (data not shown). No TUNEL-positive cells were found in scrambled antagomir-injected mice in either rostral or medial hippocampus. A single TUNEL-positive cell was present in rostral hippocampus from one miR-132 antagomir-injected mouse. In sections from the medial hippocampus, two miR-132 antagomir mice had a single TUNEL-positive cell and one mouse had two TUNEL-positive cells. These differences were not significant, compared with the scrambled antagomir group (data not shown).

Because miR-132 regulates neuronal structures both *in vitro* and *in vivo*,[24,26,45] we explored whether seizures were different in mice with depleted miR-132. Mice were injected with 0.5 nmol anti-miR-132 or scrambled antagomir injection 24 hours before induction of status epilepticus. Analysis of multiple components of the EEG recorded at the time of status epilepticus (ie, duration of high-amplitude, high-frequency discharges, EEG total power, and EEG frequency) revealed no significant differences (Figure 6, D–F).

Depletion of miR-132 Protects Hippocampal CA3 against Status Epilepticus

Last, we examined tissue sections from mice 24 hours after status epilepticus that received either 0.5 nmol of the antagomir targeting miR-132 or the scrambled version. No animals died after status epilepticus in either group. Scrambled-treated mice subjected to status epilepticus displayed typical CA3 damage in the rostral hippocampus as evidenced by FJB staining, TUNEL, and loss of NeuN staining (Figure 7, A and D). In contrast, mice injected with anti-miR-132 showed significantly fewer FJB counts, less TUNEL staining, and significantly more surviving neurons (Figure 7, A, C, and D). Analysis of the medial hippocampus showed the same protective trend (Figure 7, B and C). That is, anti-miR-132 significantly reduced FJB and TUNEL counts, and increased numbers of surviving neurons. Representative FJB, TUNEL, and NeuN staining of the medial hippocampus for each group is shown in Figure 7D.

Finally, a statistical analysis[46,47] of the relationship between seizure damage and seizure duration in scrambled and miR-132 antagomir-treated mice was performed (see Supplemental Figure S1 at *http://ajp.amjpathol.org*). The analysis revealed a significant correlation between seizure duration and seizure damage in scrambled antagomir-treated mice; this association was lost in animals injected with miR-132 antagomir. Thus, by protecting against seizure-induced neuronal death, miR-132 antagomir uncoupled the relationship between seizure duration and damage.

Discussion

In the present study, we characterized the transcriptional response of mature miRNAs to status epilepticus evoked by intra-amygdalar KA and showed this to be altered in the hippocampus of tolerant mice (ie, preconditioned animals). Compared with status epilepticus alone, miRNA expression responses in tolerance were often reduced or were regulated in the opposite direction. We also showed that *in vivo* depletion of miR-132, one of the differentially up-regulated miRNAs in injury, reduced neuronal death after status epilepticus. These findings contribute to our understanding of the molecular mechanisms of tolerance and support miRNAs as novel determinants of seizure-induced neuronal death.

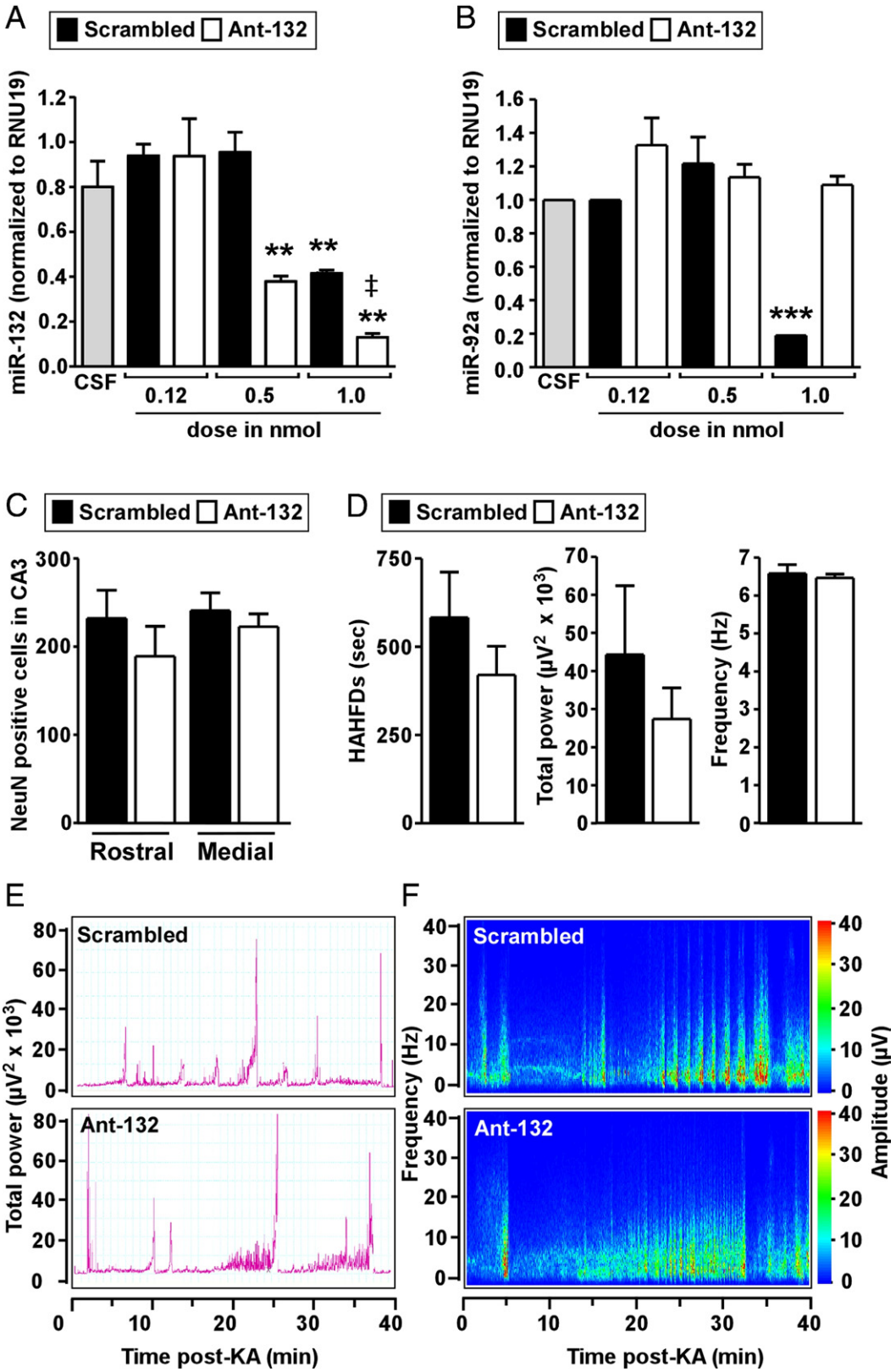

Figure 6. Effects of miR-132 antagomirs on normal brain and seizure EEG during status epilepticus. **A** and **B:** Real-time qPCR measurements of (**A**) miR-132 and (**B**) miR-92a levels in hippocampal CA3 extracts 24 hours after intracerebroventricular injection of miR-132-targeting antagomirs (Ant-132) or a nontargeting antagomir control (scrambled). $^{**}P < 0.01$ and $^{***}P < 0.0001$ versus scrambled and artificial cerebrospinal fluid (CSF); $^{‡}P < 0.05$ versus same-dose scrambled ($n = 3$ per group). **C:** NeuN counts in tissue sections at different levels of the hippocampus in animals injected 24 hours earlier with either scrambled (Scr) or the miR-132 antagomir (Ant-132) ($n = 3$ per group). **D:** EEG parameters during status epilepticus in scrambled and antagomir-132 mice ($n = 4$ to 8 per group). **E** and **F:** Frequency, amplitude and total power parameters during seizure EEG for a representative scrambled-antagomir-treated mouse and an antagomir-132-treated mouse during status epilepticus.

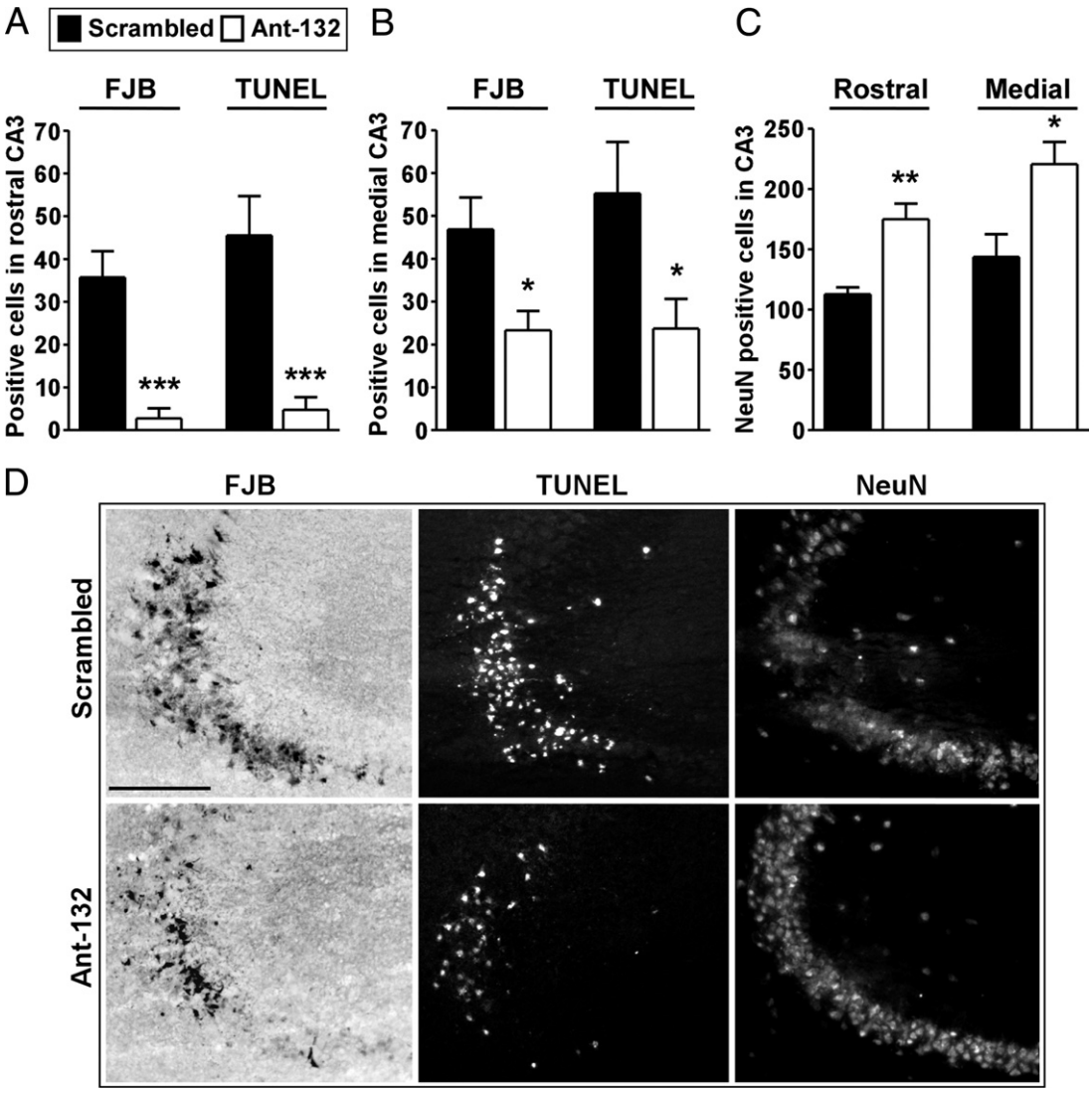

Figure 7. Depletion of miR-132 protects hippocampal CA3 against seizure-induced neuronal death. **A** and **B:** FJB and TUNEL counts 24 hours after status epilepticus for rostral (**A**), and medial hippocampus (**B**), showing the neuroprotective effect of antagomirs against miR-132 (Ant-132) compared with scrambled antagomir. **C:** NeuN counts in rostral and medial sections of hippocampus for each group. $^{*}P < 0.05$, $^{**}P < 0.01$, and $^{***}P < 0.0001$ versus scrambled antagomir. $n = 4$ to 8 per group. **D:** Representative photomicrographs of FJB, TUNEL, and NeuN staining in the ipsilateral CA3 subfield 24 hours after status epilepticus in mice injected with either scrambled or miR-132 antagomirs. Original magnification, ×20. Scale bar, 185 μm.

From initial work on single metabolites and genes,[48–51] an appreciation has emerged that tolerance is associated with large-scale, genomic reprogramming that involves altered expression of hundreds of genes.[4,5,7] The present study builds on our understanding of the molecular processes that underlie epileptic tolerance and introduces an important new contributor, namely, miRNAs. Previously, microarray analyses showed that the response of protein-coding genes in the CA3 subfield of the hippocampus to status epilepticus is profoundly altered in animals previously preconditioned by brief seizures, with widespread down-regulation, particularly of genes implicated in excitotoxicity.[8] Our present results show that status epilepticus also produces profound changes in the expression of miRNAs. Expression of more than half the detected mature miRNAs increased in the hippocampus in the injury group, indicating major transcriptional regulation of miRNAs. Because miRNAs are capable of regulating large numbers of mRNA transcripts, our data support other recent work[36,52] suggesting that miRNAs contribute to the gene expression environment of status epilepticus.

Although the mechanism by which miRNAs function differs from RNA interference, miRNAs have nevertheless been reported to directly reduce mRNA levels in cells.[53] Given that mRNAs for hundreds of protein-coding genes are reduced in epileptic tolerance relative to status epilepticus alone,[8] one prediction for the present study would have been to see greatly increased miRNA expression in tolerant animals. This was not found, however. Instead, the differential miRNA regulation in epileptic tolerance was mainly a block of the up-regulation of miRNAs after status epilepticus in combination with down-regulation of a set of miRNAs not ordinarily regulated after status epilepticus alone. Thus, the miRNA transcriptome of epileptic tolerance is most characterized by a suppression

of the normal regulated responses of miRNAs after status epilepticus.

Our immunoblotting results suggest that changes to miRNA biogenesis components are not responsible for the miRNA profile in epileptic tolerance. A necessary next step is to identify the mRNA targets targeted by miRNA changes in tolerance. This is not straightforward, and it is generally inappropriate to use exclusively bioinformatics tools predicting mRNA targets of miRNAs to identify the pathways affected and assert functional consequences, as has been reported,[52] without direct experimental validation that a particular miRNA can target an mRNA and alter translation.[31] The identification and experimental validation of the mRNA targets of the tolerance-regulated miRNAs will enable full evaluation of their potential as effectors of the neuroprotection.

How does the profile in epileptic tolerance compare to that of ischemic tolerance? Reduction of miRNA regulation is found after stroke in ischemic preconditioned mice,[11] whereas differential up-regulation of miRNAs, reported to be instigated by ischemic preconditioning,[9–11] was not a feature of epileptic tolerance. Does a set of miRNAs appear in common across these different models of tolerance? This might be expected, because there is crossover between categories of genes in ischemic and epileptic tolerance, including transport genes.[6,8] There are miRNAs down-regulated in both epileptic tolerance and ischemic tolerance, including miR-330 and miR-497. However, these are also down-regulated after status epilepticus alone, suggesting that they could not as such account for tolerance. In fact, only miR-27a appears to be regulated in the same direction in both epileptic and ischemic tolerance, with the direction opposite from its response to injury (Lusardi et al[11] and present study). However, the absence of changes in RNA-induced silencing complex uptake of miR-27a during Ago-2 analysis casts doubt on a functional influence.

It is notable that some of the mRNA and protein changes inducing the neuroprotection seen in tolerance are similar to the alterations that enable cells to evade apoptosis in cancer, such as increased Bcl-2 and polycomb group protein levels.[50,54,55] It is tempting to draw parallels again between the miRNA changes that characterize tolerance and the frequent, global down-regulation of miRNAs and their biogenesis machinery in many tumors.[56]

The present study also provides *in vivo* evidence that modulation of a seizure-regulated miRNA can influence neuropathologic outcome after status epilepticus. miR-132 has previously been reported to be expressed in mouse hippocampus,[26,29] which we also confirmed in the present study using both PCR and *in situ* hybridization. We used antagomirs to reduce hippocampal miR-132 levels, thereby modeling the tolerance-induced miR-132 profile. Antagomirs are known to function by complementary binding that leads to non-RNAi-mediated degradation of the miRNA.[43] Our present experiments showed that antagomirs targeting miR-132 profoundly reduce neuronal death within the CA3 sector after seizures. The mechanism of this protection is as yet unknown. Known targets of miR-132 include p250 GTPase-activating protein,[23] and miR-132 can promote dendritic growth and arborization in response to neuronal activity[57] and spine morphogenesis.[26] A small effect of the antagomirs on seizure duration was noted, although the present and previous[58] analyses of the statistical relationship between seizure time and damage in the model argue against this accounting for the neuroprotection. More likely, the neuroprotection relates to changes in cell death signaling pathways, rather than altered seizure severity. Of note, at least 5 of the 21 protein-coding genes differentially down-regulated in injury in our previous microarray screen[8] have predicted miR-132 binding sites within their 3′UTR (*Adrbk2*, *Grm7*, *Ntng1*, *Slc40a1* and *Vgll3*; D.H. and R.S., unpublished observations). The present study also reveals an unexpected effect of higher doses of the scrambled antagomir reducing miRNA levels of both miR-132 and the unrelated miR-92a. This observation, which may be due to off-target effects, underscores the need for full dose-response evaluation of supposedly inactive scrambled antagomirs.

Increased expression of miR-132 after status epilepticus alone was also reported after pilocarpine-induced seizures, in a CREB-dependent manner.[21] Thus, findings on this particular miRNA using the intra-amygdalar KA model can be extrapolated to other seizure models. Our data show, however, that miR-132 was not induced in the CA3 subfield in tolerance mice, nor in the CA1 that is uninjured after status epilepticus alone. Transcriptional control of miR-132 can therefore be dissociated from strong neuronal activity. Moreover, because down-regulation of miR-132 has been implicated in ischemic tolerance by enabling MECP2 protein translation,[11] and because CREB has been implicated as an effector of ischemic tolerance,[59,60] our data identify a mechanistic difference between ischemic and epileptic tolerance. We also note that miR-132 can have an anti-inflammatory role by targeting acetylcholinesterase.[61] Because inflammation and blood-brain barrier opening have been implicated in ictogenesis and epileptogenesis,[62] we cannot exclude possible favorable effects of elevated miR-132 levels in other seizure models.

Two recent studies have profiled miRNA transcriptional responses after experimental status epilepticus, but in each case miRNA was obtained from the entire hippocampus.[36,52] This limits interpretation, because of the well-established transcriptional heterogeneity among hippocampal subfields.[40,63] Indeed, we show that an individual miRNA can display large intersubfield expressional differences in the same model (Figure 5B). It is perhaps not surprising, therefore, that comparison with the findings of Liu et al,[36] who studied whole hippocampal miRNAs after systemic KA-induced seizures in rats at 24 hours, reveals no miRNAs overlapping with those reported here. We did detect some of the same miRNAs up-regulated in the study by Hu et al,[52] who profiled rats after pilocarpine-induced status epilepticus, including miR-132, miR-375, and miR-199a. These could be common seizure-regulated miRNAs. Indeed, these miRNAs were either down-regulated or unchanged after ischemia and subarachnoid hemorrhage.[11,36] Again, several miRNAs down-regulated in the study by Hu et al[52] were either

unchanged in the present study (miR-181c) or showed an opposite expression pattern (miR-29a, miR-10b, and miR-21). The present study provides a clean data set on CA3 subfield responses, one that can serve as a resource to identify a common miRNA signature among models of status epilepticus. Other strengths of the present study are the use of saline-perfused animals, which avoids potential contamination of blood miRNA in brain tissue samples.[36,52] Our qPCR-based approach offers technical advantages over microarray-based profiling in terms of greater sensitivity and specificity, and in detecting only the biologically active mature form of the miRNA.

In summary, in the present study we have characterized the mouse miRNA response in the CA3 subfield after status epilepticus evoked by intra-amygdalar KA and have shown how this is altered in previously preconditioned animals. The observed shift toward miRNA downregulation may be functionally important, and we show that targeting an injury-only up-regulated miRNA, miR-132, protected against seizure-induced neuronal death. These findings increase our understanding of the role of miRNAs in the pathogenesis of brain injury and the ability of a mild preceding seizure event to alter this response toward a state associated with tissue protection.

Acknowledgment

We thank Ronan Conroy for advice with statistical aspects of the work.

References

1. Gidday JM: Cerebral preconditioning and ischaemic tolerance. Nat Rev Neurosci 2006, 7:437–448
2. Dirnagl U, Becker K, Meisel A: Preconditioning and tolerance against cerebral ischaemia: from experimental strategies to clinical use. Lancet Neurol 2009, 8:398–412
3. Jimenez-Mateos EM, Henshall DC: Seizure preconditioning and epileptic tolerance: models and mechanisms. Int J Physiol Pathophysiol Pharmacol 2009, 1:180–191
4. Johnson MB, Simon RP: Endogenous neuroprotective mechanisms in the brain. Epilepsia 2009, 50 Suppl 12:3–4
5. Stenzel-Poore MP, Stevens SL, King JS, Simon RP: Preconditioning reprograms the response to ischemic injury and primes the emergence of unique endogenous neuroprotective phenotypes: a speculative synthesis. Stroke 2007, 38(2 Suppl):680–685
6. Stenzel-Poore MP, Stevens SL, Xiong Z, Lessov NS, Harrington CA, Mori M, Meller R, Rosenzweig HL, Tobar E, Shaw TE, Chu X, Simon RP: Effect of ischaemic preconditioning on genomic response to cerebral ischaemia: similarity to neuroprotective strategies in hibernation and hypoxia-tolerant states. Lancet 2003, 362:1028–1037
7. Koerner IP, Gatting M, Noppens R, Kempski O, Brambrink AM: Induction of cerebral ischemic tolerance by erythromycin preconditioning reprograms the transcriptional response to ischemia and suppresses inflammation. Anesthesiology 2007, 106:538–547
8. Jimenez-Mateos EM, Hatazaki S, Johnson MB, Bellver-Estelles C, Mouri G, Bonner C, Prehn JH, Meller R, Simon RP, Henshall DC: Hippocampal transcriptome after status epilepticus in mice rendered seizure damage-tolerant by epileptic preconditioning features suppressed calcium and neuronal excitability pathways. Neurobiol Dis 2008, 32:442–453
9. Dharap A, Vemuganti R: Ischemic pre-conditioning alters cerebral microRNAs that are upstream to neuroprotective signaling pathways. J Neurochem 2010, 113:1685–1691
10. Lee ST, Chu K, Jung KH, Yoon HJ, Jeon D, Kang KM, Park KH, Bae EK, Kim M, Lee SK, Roh JK: MicroRNAs induced during ischemic preconditioning. Stroke 2010, 41:1646–1651
11. Lusardi TA, Farr CD, Faulkner CL, Pignataro G, Yang T, Lan J, Simon RP, Saugstad JA: Ischemic preconditioning regulates expression of microRNAs and a predicted target, MeCP2, in mouse cortex. J Cereb Blood Flow Metab 2010, 30:744–756
12. Bartel DP: MicroRNAs: genomics, biogenesis, mechanism, and function. Cell 2004, 116:281–297
13. Lim LP, Lau NC, Garrett-Engele P, Grimson A, Schelter JM, Castle J, Bartel DP, Linsley PS, Johnson JM: Microarray analysis shows that some microRNAs downregulate large numbers of target mRNAs. Nature 2005, 433:769–773
14. Baek D, Villen J, Shin C, Camargo FD, Gygi SP, Bartel DP: The impact of microRNAs on protein output. Nature 2008, 455:64–71
15. Friedman RC, Farh KK, Burge CB, Bartel DP: Most mammalian mRNAs are conserved targets of microRNAs. Genome Res 2009, 19:92–105
16. Krol J, Loedige I, Filipowicz W: The widespread regulation of microRNA biogenesis, function and decay. Nat Rev Genet 2010, 11:597–610
17. Kim VN, Han J, Siomi MC: Biogenesis of small RNAs in animals. Nat Rev Mol Cell Biol 2009, 10:126–139
18. Peters L, Meister G: Argonaute proteins: mediators of RNA silencing. Mol Cell 2007, 26:611–623
19. Shibata M, Kurokawa D, Nakao H, Ohmura T, Aizawa S: MicroRNA-9 modulates Cajal-Retzius cell differentiation by suppressing Foxg1 expression in mouse medial pallium. J Neurosci 2008, 28:10415–10421
20. Miska EA, Alvarez-Saavedra E, Townsend M, Yoshii A, Sestan N, Rakic P, Constantine-Paton M, Horvitz HR: Microarray analysis of microRNA expression in the developing mammalian brain. Genome Biol 2004, 5:R68
21. Nudelman AS, DiRocco DP, Lambert TJ, Garelick MG, Le J, Nathanson NM, Storm DR: Neuronal activity rapidly induces transcription of the CREB-regulated microRNA-132, in vivo. Hippocampus 2010, 20:492–498
22. Wibrand K, Panja D, Tiron A, Ofte ML, Skaftnesmo KO, Lee CS, Pena JT, Tuschl T, Bramham CR: Differential regulation of mature and precursor microRNA expression by NMDA and metabotropic glutamate receptor activation during LTP in the adult dentate gyrus in vivo. Eur J Neurosci 2010, 31:636–645
23. Vo N, Klein ME, Varlamova O, Keller DM, Yamamoto T, Goodman RH, Impey S: A cAMP-response element binding protein-induced microRNA regulates neuronal morphogenesis [Erratum appeared in Proc Natl Acad Sci USA 2006, 103:825]. Proc Natl Acad Sci USA 2005, 102:16426–16431
24. Schratt GM, Tuebing F, Nigh EA, Kane CG, Sabatini ME, Kiebler M, Greenberg ME: A brain-specific microRNA regulates dendritic spine development [Erratum in Nature 2006, 441:902]. Nature 2006, 439:283–289
25. Siegel G, Obernosterer G, Fiore R, Oehmen M, Bicker S, Christensen M, Khudayberdiev S, Leuschner PF, Busch CJ, Kane C, Hubel K, Dekker F, Hedberg C, Rengarajan B, Drepper C, Waldmann H, Kauppinen S, Greenberg ME, Draguhn A, Rehmsmeier M, Martinez J, Schratt GM: A functional screen implicates microRNA-138-dependent regulation of the depalmitoylation enzyme APT1 in dendritic spine morphogenesis. Nat Cell Biol 2009, 11:705–716
26. Edbauer D, Neilson JR, Foster KA, Wang CF, Seeburg DP, Batterton MN, Tada T, Dolan BM, Sharp PA, Sheng M: Regulation of synaptic structure and function by FMRP-associated microRNAs miR-125b and miR-132 [Erratum appeared in Neuron 2010, 68:161]. Neuron 2010, 65:373–384
27. Schaefer A, O'Carroll D, Tan CL, Hillman D, Sugimori M, Llinas R, Greengard P: Cerebellar neurodegeneration in the absence of microRNAs. J Exp Med 2007, 204:1553–1558
28. Hébert SS, De Strooper B: Alterations of the microRNA network cause neurodegenerative disease. Trends Neurosci 2009, 32:199–206
29. Konopka W, Kiryk A, Novak M, Herwerth M, Parkitna JR, Wawrzyniak M, Kowarsch A, Michaluk P, Dzwonek J, Arnsperger T, Wilczynski G, Merkenschlager M, Theis FJ, Kohr G, Kaczmarek L, Schutz G: MicroRNA loss enhances learning and memory in mice. J Neurosci 2010, 30:14835–14842
30. Eacker SM, Dawson TM, Dawson VL: Understanding microRNAs in neurodegeneration. Nat Rev Neurosci 2009, 10:837–841

31. Saugstad JA: MicroRNAs as effectors of brain function with roles in ischemia and injury, neuroprotection, and neurodegeneration. J Cereb Blood Flow Metab 2010, 30:1564–1576
32. Hatazaki S, Bellver-Estelles C, Jimenez-Mateos EM, Meller R, Bonner C, Murphy N, Matsushima S, Taki W, Prehn JH, Simon RP, Henshall DC: Microarray profile of seizure damage-refractory hippocampal CA3 in a mouse model of epileptic preconditioning. Neuroscience 2007, 150:467–477
33. Paxinos G, Franklin KBJ: The mouse brain in stereotaxic coordinates, ed 2. San Diego, Elsevier, 2001
34. Murphy BM, Engel T, Paucard A, Hatazaki S, Mouri G, Tanaka K, Tuffy LP, Jimenez-Mateos EM, Woods I, Dunleavy M, Bonner HP, Meller R, Simon RP, Strasser A, Prehn JH, Henshall DC: Contrasting patterns of Bim induction and neuroprotection in Bim-deficient mice between hippocampus and neocortex after status epilepticus. Cell Death Differ 2010, 17:459–468
35. Engel T, Hatazaki S, Tanaka K, Prehn JH, Henshall DC: Deletion of Puma protects hippocampal neurons in a model of severe status epilepticus. Neuroscience 2010, 168:443–450
36. Liu DZ, Tian Y, Ander BP, Xu H, Stamova BS, Zhan X, Turner RJ, Jickling G, Sharp FR: Brain and blood microRNA expression profiling of ischemic stroke, intracerebral hemorrhage, and kainate seizures. J Cereb Blood Flow Metab 2010, 30:92–101
37. Shibata M, Nakao H, Kiyonari H, Abe T, Aizawa S: MicroRNA-9 regulates neurogenesis in mouse telencephalon by targeting multiple transcription factors. J Neurosci 2011, 31:3407–3422
38. Engel T, Murphy BM, Hatazaki S, Jimenez-Mateos EM, Concannon CG, Woods I, Prehn JH, Henshall DC: Reduced hippocampal damage and epileptic seizures after status epilepticus in mice lacking proapoptotic Puma. FASEB J 2010, 24:853–861
39. Jimenez-Mateos EM, Mouri G, Conroy RM, Henshall DC: Epileptic tolerance is associated with enduring neuroprotection and uncoupling of the relationship between CA3 damage, neuropeptide Y rearrangement and spontaneous seizures following intra-amygdalar kainic acid-induced status epilepticus in mice. Neuroscience 2010, 171:556–565
40. Lein ES, Zhao X, Gage FH: Defining a molecular atlas of the hippocampus using DNA microarrays and high-throughput in situ hybridization. J Neurosci 2004, 24:3879–3889
41. Magill ST, Cambronne XA, Luikart BW, Lioy DT, Leighton BH, Westbrook GL, Mandel G, Goodman RH: microRNA-132 regulates dendritic growth and arborization of newborn neurons in the adult hippocampus. Proc Natl Acad Sci USA 2010, 107:20382–20387
42. Krützfeldt J, Rajewsky N, Braich R, Rajeev KG, Tuschl T, Manoharan M, Stoffel M: Silencing of microRNAs in vivo with 'antagomirs'. Nature 2005, 438:685–689
43. Krützfeldt J, Kuwajima S, Braich R, Rajeev KG, Pena J, Tuschl T, Manoharan M, Stoffel M: Specificity, duplex degradation and subcellular localization of antagomirs. Nucleic Acids Res 2007, 35:2885–2892
44. Elmén J, Lindow M, Schütz S, Lawrence M, Petri A, Obad S, Lindholm M, Hedtjärn M, Hansen HF, Berger U, Gullans S, Kearney P, Sarnow P, Straarup EM, Kauppinen S: LNA-mediated microRNA silencing in non-human primates. Nature 2008, 452:896–899
45. Christensen M, Larsen LA, Kauppinen S, Schratt G: Recombinant adeno-associated virus-mediated microRNA delivery into the postnatal mouse brain reveals a role for miR-134 in dendritogenesis in vivo. Front Neural Circuits 2010, 3:16
46. Verardi V, Croux C: Robust regression in Stata. Stata J 2009, 9:439–453
47. Yohai VJ: High breakdown point and high efficiency robust estimators for regression. Ann Stat 1987, 15:642–656
48. Heurteaux C, Lauritzen I, Widmann C, Lazdunski M: Essential role of adenosine, adenosine A1 receptors, and ATP-sensitive K+ channels in cerebral ischemic preconditioning. Proc Natl Acad Sci USA 1995, 92:4666–4670
49. Chen J, Graham SH, Zhu RL, Simon RP: Stress proteins and tolerance to focal cerebral ischemia. J Cereb Blood Flow Metab 1996, 16:566–577
50. Shimizu S, Nagayama T, Jin KL, Zhu L, Loeffert JE, Watkins SC, Graham SH, Simon RP: bcl-2 Antisense treatment prevents induction of tolerance to focal ischemia in the rat brain. J Cereb Blood Flow Metab 2001, 21:233–243
51. McLaughlin B, Hartnett KA, Erhardt JA, Legos JJ, White RF, Barone FC, Aizenman E: Caspase 3 activation is essential for neuroprotection in preconditioning. Proc Natl Acad Sci USA 2003, 100:715–720
52. Hu K, Zhang C, Long L, Long X, Feng L, Li Y, Xiao B: Expression profile of microRNAs in rat hippocampus following lithium-pilocarpine-induced status epilepticus. Neurosci Lett 2011, 488:252–257
53. Guo H, Ingolia NT, Weissman JS, Bartel DP: Mammalian microRNAs predominantly act to decrease target mRNA levels. Nature 2010, 466:835–840
54. Stapels M, Piper C, Yang T, Li M, Stowell C, Xiong ZG, Saugstad J, Simon RP, Geromanos S, Langridge J, Lan JQ, Zhou A: Polycomb group proteins as epigenetic mediators of neuroprotection in ischemic tolerance. Sci Signal 2010, 3:ra15
55. Mills AA: Throwing the cancer switch: reciprocal roles of polycomb and trithorax proteins. Nat Rev Cancer 2010, 10:669–682
56. Calin GA, Croce CM: MicroRNA signatures in human cancers. Nat Rev Cancer 2006, 6:857–866
57. Wayman GA, Davare M, Ando H, Fortin D, Varlamova O, Cheng HY, Marks D, Obrietan K, Soderling TR, Goodman RH, Impey S: An activity-regulated microRNA controls dendritic plasticity by down-regulating p250GAP. Proc Natl Acad Sci USA 2008, 105:9093–9098
58. Murphy B, Dunleavy M, Shinoda S, Schindler C, Meller R, Bellver-Estelles C, Hatazaki S, Dicker P, Yamamoto A, Koegel I, Chu X, Wang W, Xiong Z, Prehn J, Simon R, Henshall D: Bcl-w protects hippocampus during experimental status epilepticus. Am J Pathol 2007, 171:1258–1268
59. Hara T, Hamada J, Yano S, Morioka M, Kai Y, Ushio Y: CREB is required for acquisition of ischemic tolerance in gerbil hippocampal CA1 region. J Neurochem 2003, 86:805–814
60. Meller R, Minami M, Cameron JA, Impey S, Chen D, Lan JQ, Henshall DC, Simon RP: CREB-mediated Bcl-2 protein expression after ischemic preconditioning. J Cereb Blood Flow Metab 2005, 25:234–246
61. Shaked I, Meerson A, Wolf Y, Avni R, Greenberg D, Gilboa-Geffen A, Soreq H: MicroRNA-132 potentiates cholinergic anti-inflammatory signaling by targeting acetylcholinesterase. Immunity 2009, 31:965–973
62. Vezzani A, French J, Bartfai T, Baram TZ: The role of inflammation in epilepsy. Nat Rev Neurol 2011, 7:31–40
63. Greene JG, Borges K, Dingledine R: Quantitative transcriptional neuroanatomy of the rat hippocampus: evidence for wide-ranging, pathway-specific heterogeneity among three principal cell layers. Hippocampus 2009, 19:253–264